

# Bluetooth Performance in the Presence of 802.11b WLAN

Ivan Howitt, *Member, IEEE*

**Abstract**—Both Bluetooth and 802.11b wireless communication technology are poised to make a significant impact in many applications. The complementary nature of the two technologies leads to applications enhanced by their collocation and simultaneous operation. Thus heightening the need for understanding the coexistence issues between the two technologies. A method was developed for evaluating the impact an 802.11b network will have on the Bluetooth piconet performance. A three step process was used in this development: characterize the 802.11b interference in a stationary environment, characterize the Bluetooth performance in the presence of a single 802.11b interferer and characterize the Bluetooth performance in an arbitrary 802.11b network environment. Empirical results were used to develop and substantiate the analytical model. The root-mean-square (RMS) difference between the single interferer empirical test results and the analytical model results was 2%. Analysis results, based on a specific range of radio propagation parameters and 802.11b network parameters, are presented.

**Index Terms**—802.11b, bluetooth, coexistence, WLAN, WPAN.

## I. INTRODUCTION

THE Bluetooth wireless communication technology [1], [2] is poised to make a significant impact in many applications. The activity surrounding the technology underlies its need in the community, but also foreshadows the need to understand the impact current wireless services operating in the same unlicensed (UL) band will have on Bluetooth piconet performance. Both Bluetooth wireless personal area networks (WPAN) and 802.11b wireless local area networks (WLANs) share the same 2.4 GHz UL frequency band and provide complementary wireless solutions for connectivity. This complementary nature of the two services could enhance the use of both protocols at the same physical location and provide an incentive for their adoption. However, the issues surrounding their coexistence need to be addressed, prior to the interoperability problems, whether speculative or actual, become a deterrent to their commercial acceptance.

Coexistence analysis between the 802.11b and Bluetooth piconet has been addressed in [3]–[9]. The paper by Haartsen and Zurbes [8] examines the impact an 802.11b network will have on Bluetooth performance and the remaining references examine the impact Bluetooth piconets will have on the 802.11b network. The approach used in [8] was based on a combination of analytical and Monte Carlo simulations for a specific network con-

figuration. Their analysis provides insight, but their approach does not provide a general method for examining the coexistence issue.

The goal of the research presented in this paper is to provide an analytical model for evaluating the coexistence issue where the analytical model results are tested for consistency against empirical test results. The coexistence issue addressed is the impact an 802.11b will have on Bluetooth performance, under various scenarios. A three step approach was used in developing the analytical model:

- 1) Characterize 802.11b interference under static conditions, i.e., 802.11b interference and Bluetooth signals remain stationary.
- 2) Characterize Bluetooth performance when collocated with a single 802.11b signal source.
- 3) Characterize Bluetooth performance when operating in an arbitrary 802.11b network environment.

The analytical models developed for Steps 1 and 2 were compared with empirical test results in order to substantiate the model. In Section II, the measures of performance for the Bluetooth network are derived in terms of the probability of collision between the 802.11b interference signal and the desired Bluetooth piconet signal. Next, the 802.11b interference is characterized based on empirical test results in Section III. This characterization establishes the basis for the analytical models in the following sections. In Section IV and V, the analytical models for Bluetooth performance in a single 802.11b environment and in an arbitrary 802.11b network environment are derived, respectively. Bluetooth performance analysis results are presented in Section VI and conclusions are given in Section VII.

## II. MEASURE OF PERFORMANCE IN INTERFERENCE ENVIRONMENT

Bluetooth network performance can be evaluated from a number of viewpoints using various measures of performance (MOPs). The relevance of each MOP is dependent upon the specific network requirements. In this paper, the Bluetooth network performance is based on packet error rate (PER). In this section, an expression for the PER MOP is derived in terms of the probability of collision,  $\Pr[C]$ . A collision,  $C$ , defines the event where one or more 802.11b signals corrupt a Bluetooth data packet, such that retransmission of the data packet is required. The derivation of  $\Pr[C]$  is presented in Section III through Section V. Other network MOPs, such as packet latency, can also be evaluated using the same approach as the author derived in [3], for the analysis of the impact of Bluetooth on 802.11b.

Manuscript received July 31, 2001; revised March 27, 2002. This work was supported by Eaton Corporation Innovation Center.

The author is with the Wireless & Signal Processing Laboratory, Electrical Engineering & Computer Science Department, University of Wisconsin, Milwaukee, WI 53201 USA (e-mail: howitt@uwm.edu).

Digital Object Identifier 10.1109/TVT.2002.804853

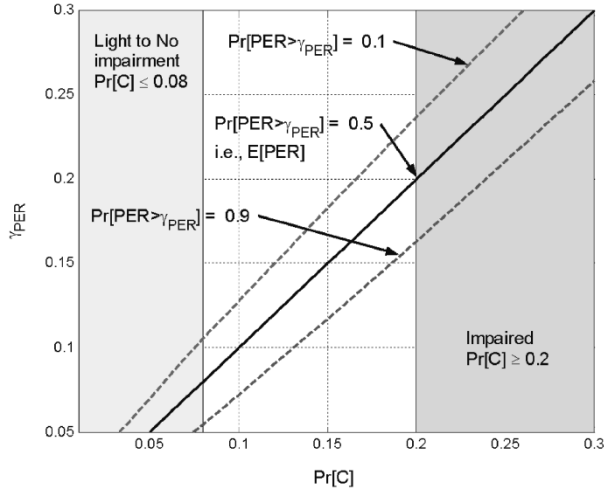


Fig. 1. MOP, curves of equal PER probability, in terms of  $\Pr[C]$ .

Given  $N$  Bluetooth packets are transmitted and assuming the packet collisions with 802.11b are independent and identically distributed (iid), then the PER is a random variable (RV) that can be expressed as a function of  $\Pr[C]$ . The probability the PER exceeds a PER threshold,  $\gamma_{PER}$ , can be modeled by a binomial distribution [10]

$$\Pr[PER > \gamma_{PER}] = 1 - \Pr[PER \leq \gamma_{PER}]$$

$$\Pr[PER \leq \gamma_{PER}] = \sum_{n=0}^{N \times \gamma_{PER}} \binom{N}{n} (\Pr[C])^n (1 - \Pr[C])^{N-n} \quad (1)$$

where, for ease of notation,  $\gamma_{PER} \in [0/N, 1/N, \dots, N/N]$ . A Gaussian approximation to the binomial distribution [11] can be used to estimate (1), given  $N$  is sufficiently large, such that,  $N \times \Pr[C] \gg 1$ ,

$$\Pr[PER > \gamma_{PER}] \cong \frac{1}{2} - \frac{1}{2} \operatorname{erf} \left( \frac{N(\gamma_{PER} - \Pr[C])}{\sqrt{2\gamma_{PER}N\Pr[C](1 - \Pr[C])}} \right) \quad (2)$$

where  $\operatorname{erf}(\cdot)$  is the standard error function. In Fig. 1, graphs of equal probability for  $\Pr[PER > \gamma_{PER}]$  are depicted based on (2).

A common network performance specification is based on the expected PER,  $E[PER]$ . From both (1) and (2), it is straightforward to obtain  $E[PER] = \Pr[C]$ . As illustrated in Fig. 1,  $E[PER] \leq 0.08$  is used to define an upper bound on  $\Pr[C]$ . Under this condition, it is assumed little or no Bluetooth network impairment is observed. However, the network is assumed to be impaired, if  $E[PER] \geq 0.2$ . Both of these bounds were selected for illustrative purposes. Actual bounds on the MOP will be application dependent. The goal of the paper is to provide a method for assessing the MOP over the variations in an application's operational environment where the application has specific communication requirements based on using the Bluetooth protocol.

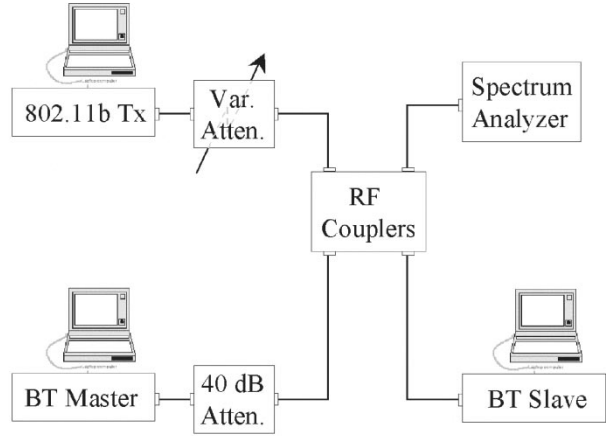


Fig. 2. Test setup for empirical measurements.

### III. CHARACTERIZATION OF IEEE 802.11B INTERFERENCE

Characterizing the interference power to signal power threshold,  $\gamma$ , at which a packet's retransmission is likely to be required, is presented in this section. That is, if  $\Omega_{I/S} \geq \gamma$ , then the event  $C$  occurs where  $\Omega_{I/S}$  is the received interference to signal power at the input to the Bluetooth receiver. As indicated in [3], [12], characterizing  $\gamma$  for both cochannel and adjacent channel interference is essential, in order to effectively characterize  $\Pr[C]$ . Therefore,  $\gamma(f_{\text{offset}})$  is dependent on the carrier frequency offset,  $f_{\text{offset}}$ , where  $f_{\text{offset}}$  is the frequency separation between the Bluetooth carrier frequency and the 802.11b carrier frequency. An empirical study was conducted in order to characterize  $\gamma(f_{\text{offset}})$  and based on the data collected an analytical model of  $\gamma(f_{\text{offset}})$  was determined. The analytical model presented below is an extension of the model presented in [12].

The test setup used for the empirical measurements is depicted in Fig. 2. The Bluetooth Master and Slave were based on Ericsson Bluetooth starter kit, compliant with version 1.1 of the Bluetooth specification. The Bluetooth signal was attenuated such that the signal at the Bluetooth slave was within the desired power level of the receiver,  $-48.5$  dBm. The Bluetooth slave was the system under test and the  $E[PER]$  was estimated based on variations of the interference signal power and  $f_{\text{offset}}$ . The IEEE 802.11b interference signal was generated using IEEE 802.11b compliant Tx (Prism II) with continuous transmission and the desired interference to signal ratio (I/S) was obtained by setting a variable attenuator in the interference signal path. In order to estimate  $E[PER]$ ,  $10^3$  trials for each scenario were evaluated where a scenario was based on using a specific  $f_{\text{offset}}$ ,  $\Omega_{I/S}$  and Bluetooth packet type. The Bluetooth packet type determines the Bluetooth packet timing as well as the forward error correction (FEC) used on the packet payload [2]. For the study presented in the paper a dh1 packet type was used and therefore the payload has no FEC and the relevant packet timing is given in Table I. Table I contains definitions and values for the parameters used throughout the paper.

The empirical test results were used to estimate the  $E[PER]$  or as presented in Section II,  $E[PER] = \Pr[C]$ . The empirical results provide an estimate of the likelihood the  $\Omega_{I/S}$  is sufficient to cause a collision at a given  $f_{\text{offset}}$ . Since, a

TABLE I  
PARAMETER DEFINITIONS AND VALUES

	Parameter	Definition	Value or Range
Bluetooth Parameters	$\tau_H$	Access code & header transmission time	126 $\mu$ s
	$\tau_{BT}$	Packet transmission time	366 $\mu$ s
	$\Omega_{BT}$	Transmit power	0 dBm
	$d_s$	Transmitter to receiver separation	0.5 to 9.5 m
	$B_{eq}$	Equivalent noise bandwidth	0.81 MHz
	IEEE 802.11b Parameters	$T_p$	Packet transmission time
$T_{ACK}$		Acknowledgement transmission time	106 $\mu$ s
$T_{p02}$		Packet period	Single Interferer: 1580 $\mu$ s Network: 1676 $\mu$ s
$B_{002}$		Transmission bandwidth	17.6 MHz
$\Omega_{002}$		Transmit power	20 dBm
$d_{AP}$		Access point coverage radius	15 to 20 m
$D_{STA}$		Station density	0.02 to 0.1 STA/m <sup>2</sup>
$D_{AP}$		Access point density	1/ $\pi d_{AP}^2$ AP/m <sup>2</sup>
$G$		Offered traffic to each access point	0.01 to 1 Erlang
$R$		Fraction of downlink packet transmission	0 to 1
Environment Parameters	$n$	Path loss exponent	2 to 4
	$\sigma_{I/S}$	Interference to signal shadowing standard deviation	5 to 11 dB
	$B_{UL}$	Nominal 2.4GHz UL band bandwidth	80 MHz

collision is solely dependent on the power threshold  $\gamma(f_{\text{offset}})$  at which  $\Omega_{I/S} \geq \gamma(f_{\text{offset}})$ , the empirical test result provide an estimate of  $\Pr[C|f_{\text{offset}}] = \Pr[\gamma(f_{\text{offset}}) \leq \Omega_{I/S}|f_{\text{offset}}]$  where  $\gamma(f_{\text{offset}})$  is a RV dependent on both  $f_{\text{offset}}$  and  $\Omega_{I/S}$ . The empirical tests were therefore used to estimate the conditional cumulative distribution function (cdf) of  $\gamma(f_{\text{offset}})$ ,  $F_E[\gamma(f_{\text{offset}})|f_{\text{offset}}] = \Pr[\gamma(f_{\text{offset}}) \leq \Omega_{I/S}|f_{\text{offset}}]$ . These results are illustrated in Fig. 3 where  $F_E[\gamma(f_{\text{offset}})|f_{\text{offset}} = 5 \text{ MHz}]$  is graphed based on empirical test results. From the graph in Fig. 3, note  $\Pr[\gamma(f_{\text{offset}}) \leq \Omega_{I/S}|f_{\text{offset}} = 5 \text{ MHz}] = 0.06$  occurs at  $\Omega_{I/S} \approx -10 \text{ dB}$  and  $\Pr[\gamma(f_{\text{offset}}) \leq \Omega_{I/S}|f_{\text{offset}} = 5 \text{ MHz}] = 0.90$  occurs at  $\Omega_{I/S} \approx -2 \text{ dB}$ . In Fig. 4, contours of these two probabilities (0.06 and 0.90) are graphed for  $F_E[\gamma(f_{\text{offset}})|f_{\text{offset}}]$  over the range of  $f_{\text{offset}}$  and  $\Omega_{I/S}$  tested experimentally.

Based on the empirical data, the following analytical model was determined

$$\gamma(f_{\text{offset}}) = \hat{\gamma} - J_S(f_{\text{offset}}) + \chi_\gamma \text{ (dB)} \quad (3)$$

where  $\hat{\gamma}$  is a constant,  $J_S(f_{\text{offset}})$  is the normalized interference suppression and  $\chi_\gamma$  is a zero mean Gaussian distributed RV with standard deviation  $\sigma_\gamma$ . Both  $\hat{\gamma}$  and  $\sigma_\gamma$  were estimated from the empirical data with  $\hat{\gamma} = -7.69 \text{ dB}$  and  $\sigma_\gamma = 2.45 \text{ dB}$ . Determining the portion of the 802.11b energy within the passband of the Bluetooth Gaussian filter provides

$$J_S(f_{\text{offset}}) = 10 \log_{10} \left( \frac{\int_0^\infty G_S(f) |H_{BT}(f - f_{\text{offset}})|^2 df}{\int_0^\infty G_S(f) |H_{BT}(f)|^2 df} \right) \text{ (dB)} \quad (4)$$

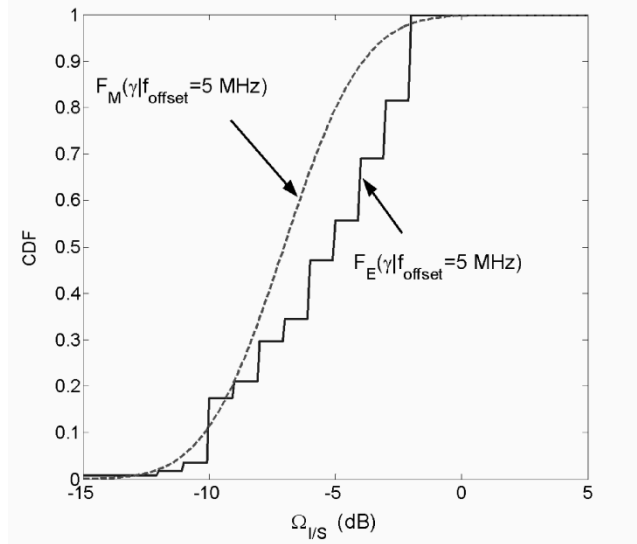


Fig. 3. Comparison of cdfs of  $\gamma(f_{\text{offset}})$  based on analytical model,  $F_M(\gamma(f_{\text{offset}})|f_{\text{offset}} = 5 \text{ MHz})$  and empirical test results,  $F_E(\gamma(f_{\text{offset}})|f_{\text{offset}} = 5 \text{ MHz})$ .

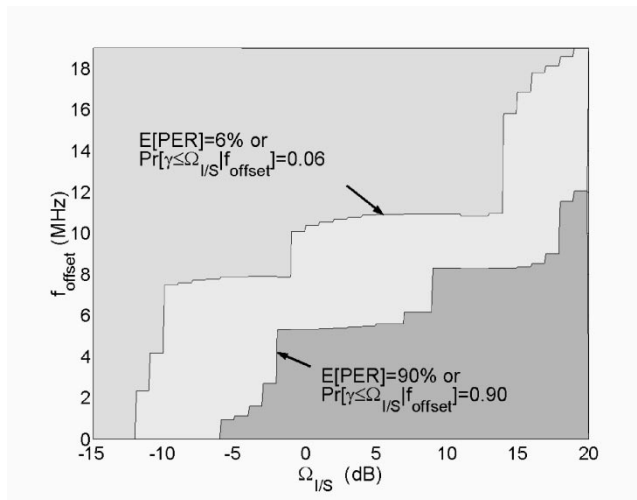


Fig. 4. Contour plot based on empirical data,  $E[PER]$  versus  $f_{\text{offset}}$  and  $\Omega_{I/S}$ . Graph can also be interpreted as the conditional cdf of  $\gamma(f_{\text{offset}})$ .

where  $G_S(f)$  is the power spectral density (PSD) of the 802.11b transmit signal,  $s(t)$ . The transmit signal is modeled by

$$s(t) = \Psi_{PA}(g_{OBO}(h_{802}(t)^*x(t))) \quad (5)$$

where  $x(t)$  is an 11 MHz chip rate QPSK signal and  $h_{802}(t)$  is a 5th order Butterworth filter with cutoff frequency of 8.8 MHz. The function  $\Psi_{PA}(\cdot)$ , in conjunction with  $g_{OBO}$ , models the effects of the 802.11b transmit power amplifier [13], where  $g_{OBO}$  is the output backoff from full saturation and

$$\Psi_{PA}(Ae^{j\phi}) = \left( \frac{A}{(1 + A^{2p})^{1/2p}} \right) e^{j\phi}. \quad (6)$$

A graph of  $J_S(f_{\text{offset}})$  is shown in Fig. 5 with  $g_{OBO} = -3.5 \text{ dB}$  and  $p = 2$ .

For comparison purposes the conditional cdf of  $\gamma(f_{\text{offset}})$  based on (3),  $F_M[\gamma|f_{\text{offset}}]$ , with  $f_{\text{offset}} = 5 \text{ MHz}$  is depicted in Fig. 3. The contours of  $F_M[\gamma|f_{\text{offset}}] = 0.06$  and

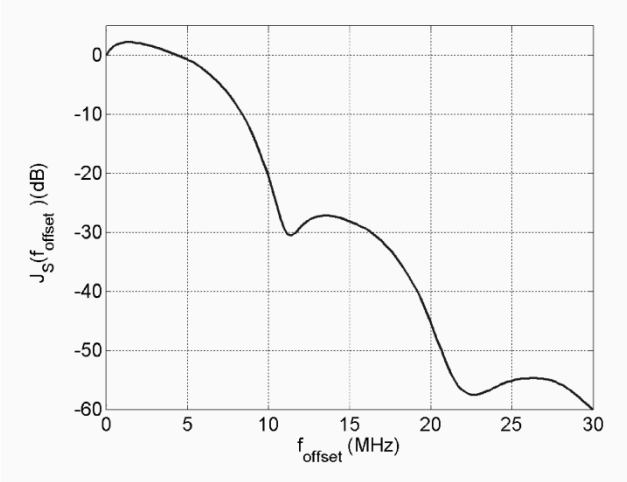


Fig. 5. Normalized Bluetooth interference suppression versus frequency offset, based on 802.11b interference.

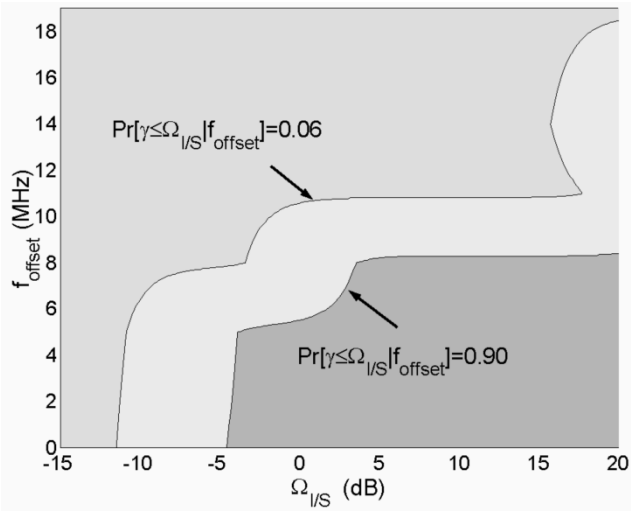


Fig. 6. Contour plot of the cdf of  $\gamma(f_{\text{offset}})$  based on the analytical model.

$F_M[\gamma|f_{\text{offset}}] = 0.90$  are graphed in Fig. 6. Since  $\gamma(f_{\text{offset}})$  is a two dimensional RV, a generalization of the K-S test [14] motivated a method for comparing the two cdfs. The cdfs,  $F_E[\gamma(f_{\text{offset}})]$  and  $F_M[\gamma(f_{\text{offset}})]$ , were determined based on the conditional cdfs, under the assumption  $f_{\text{offset}}$  is a uniform RV independent of  $\Omega_{I/S}$ . The similarity between the two distributions was evaluated using

$$D = \max_{(\Omega_{I/S}, f_{\text{offset}}) \in A} \left( \left| F_E[\gamma(f_{\text{offset}})|A] - F_M[\gamma(f_{\text{offset}})|A] \right| \right). \quad (7)$$

Using  $A$  corresponding to the range of  $(\Omega_{I/S}, f_{\text{offset}})$  evaluated empirically,  $D = 0.23$ .

#### IV. COEXISTENCE IN A SINGLE INTERFERER ENVIRONMENT

Based on the analytical model developed for  $\gamma(f_{\text{offset}})$ , (3), a stochastic model is derived to evaluate  $\Pr[C]$ . The scenario evaluated in this section is based on a single 802.11b interference source. The analytical model is derived such that the comparison to empirical results obtained from a consistent set of tests

is feasible. The empirical tests were based on a test setup similar to the one presented in Section III, Fig. 2. The Bluetooth Master and Slave transmitted dh1 packets based on a pseudo-random frequency hopping pattern. The 802.11b interferer was periodically transmitting packets with a fixed transmission duration,  $T_P = 850 \mu\text{s}$  and an interframe spacing on average of  $730 \mu\text{s}$ . The variable attenuator in the interference path was adjusted to set  $\Omega_{I/S}$ .

The single interferer analytical model is based on evaluating  $\Pr[C]$  under the following conditions for a collision. A collision occurs when the Bluetooth signal and the 802.11b signal are time coincident and the interference to signal ratio is sufficient to cause the Bluetooth packet to be corrupted based on the carrier offset between the two signals. Using the results from Section III, the probability of collision for a single 802.11b interferer is

$$\Pr[C] = \int_{-\infty}^{\infty} \int_{-\infty}^{\infty} \Pr[C|\gamma, f_{\text{offset}}] \cdot f_{\gamma}(\gamma|f_{\text{offset}}) f_{f_{\text{offset}}}(f_{\text{offset}}) d\gamma df_{\text{offset}}. \quad (8)$$

where  $f_{\gamma}(\gamma|f_{\text{offset}})$  is the conditional probability density function (pdf) of  $\gamma$ ,  $f_{f_{\text{offset}}}(\cdot)$  is the pdf of  $f_{\text{offset}}$  and  $\Pr[C|\gamma, f_{\text{offset}}]$  is the conditional probability of collision given  $\gamma$  and  $f_{\text{offset}}$ . The Bluetooth physical layer protocol is based on frequency hopping where the hopping pattern is pseudo-random over 79 nonoverlapping 1 MHz frequency bands. Since the hopping pattern is uniform over the UL Band,  $f_{\text{offset}}$  is modeled as a uniform RV with  $f_{\text{offset}} \in [-B_{UL}/2, \dots, 0, \dots, B_{UL}/2]$ ,

$$f_{f_{\text{offset}}}(f_{\text{offset}}) = \begin{cases} \frac{1}{B_{UL}} & -\frac{B_{UL}}{2} \leq f_{\text{offset}} < \frac{B_{UL}}{2} \\ 0 & \text{o.w.} \end{cases} \quad (9)$$

where  $B_{UL} = 80$  MHz is the UL bandwidth. Equation (9) assumes a worst case interference scenario with the 802.11b carrier frequency centered within the UL band. Based on (3),  $f_{\gamma}(\gamma|f_{\text{offset}})$  is a Gaussian pdf with mean  $\bar{\gamma}(f_{\text{offset}}) = \hat{\gamma} - J_S(f_{\text{offset}})$  and variance  $\sigma_{\gamma}^2$ .

Since a collision occurs when the Bluetooth signal and the 802.11b interference signal are time coincident and  $\Omega_{I/S} \geq \gamma(f_{\text{offset}})$ , the conditional probability of collision is

$$\Pr[C|\gamma, f_{\text{offset}}] = \begin{cases} \Pr[C_T] & \Omega_{I/S} \geq \gamma(f_{\text{offset}}) \\ 0 & \Omega_{I/S} < \gamma(f_{\text{offset}}) \end{cases} \quad (10)$$

where  $\Pr[C_T]$  is the probability of time coincidence between the 802.11b and Bluetooth packets. Note, for the single interference environment,  $\Omega_{I/S}$  is an independent variable of the analysis and is not a RV.

Using the symmetry of  $f_{f_{\text{offset}}}(\cdot)$  and substituting (9) and (10) into (8)

$$\Pr[C] = \frac{2\Pr[C_T]}{B_{UL}} \int_0^{B_{UL}/2} \int_{-\infty}^{\Omega_{I/S}} f_{\gamma}(\gamma|f_{\text{offset}}) d\gamma df_{\text{offset}} \quad (11)$$

and evaluating the inner integral

$$\Pr[C] = \frac{2\Pr[C_T]}{B_{UL}} \int_0^{B_{UL}/2} \left( 1 - \frac{1}{2} \cdot \left[ \text{erfc} \left( \frac{\Omega_{I/S} - \bar{\gamma}(f_{\text{offset}})}{\sqrt{2}\sigma_{\gamma}} \right) \right] \right) df_{\text{offset}} \quad (12)$$

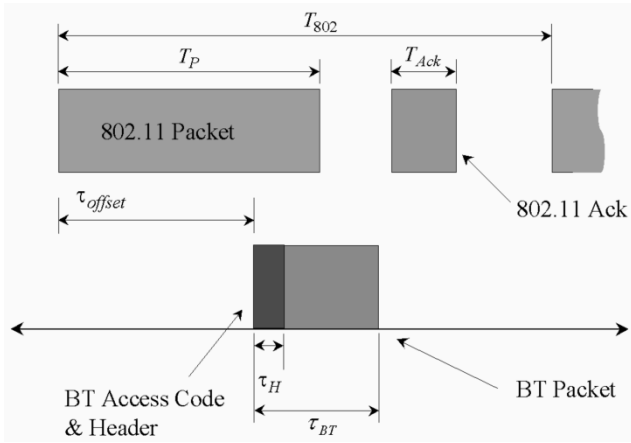


Fig. 7. Relative timing between Bluetooth Tx time slots and 802.11 packet.

where  $\text{erfc}(\cdot)$  is the complementary error function. The integral in (12) was numerically estimated in order to evaluate  $\Pr[C]$ .

The probability the signals are time coincident,  $\Pr[C_T]$ , is based on the relative timing between the Bluetooth and 802.11b signals, as illustrated in Fig. 7. For the 802.11b, a packet transmission,  $T_P$ , from source to destination, is followed by an acknowledgment,  $T_{Ack}$ , from destination to source. In order to maintain consistency with the empirical testing, time coincidence occurred when the 802.11b and Bluetooth packet transmissions were overlapping in time. A collision due to 802.11b acknowledgment (Ack) signal or a corrupted Bluetooth Ack signal are not considered for the single interferer analytical model. In addition, the time period between 802.11b packet transmissions,  $T_{802}$ , for the single interferer empirical test was measured to be on average  $T_{802} = 1580 \mu\text{s}$ . The Bluetooth packet timing is divided into the packet transmission time,  $\tau_{BT}$  and the time required to transmit the Bluetooth access code and header,  $\tau_H$ . A more general formulation is presented in Section V for evaluating the coexistence in an 802.11b network interference environment. From Fig. 7,  $\tau_{\text{offset}}$  is the time offset between an 802.11b packet and Bluetooth packet. Modeling  $\tau_{\text{offset}}$  as a uniform RV with  $\tau_{\text{offset}} \in [0, \dots, T_{802}]$ , then the event  $C_T$  occurs when  $\tau_{\text{offset}} \in [0, \dots, T_P] \cup [T_{802} - \tau_{BT}, \dots, T_{802}]$  and therefore

$$\Pr[C_T] = \min \left[ \frac{T_P + \tau_{BT}}{T_{802}}, 1 \right] \quad (13)$$

where  $\tau_{BT} = 366 \mu\text{s}$  for consistency with the empirical tests. The formulation of (13) assumes a collision occurs given the two signals are time coincident for any time duration greater than zero. This is justified since the Bluetooth symbol interval is short compared to the 802.11b packet duration.

Fig. 8 provides a comparison between the analytical model and empirical results for  $\Pr[C]$ . The analytical results are based on substituting (13) into (12) and numerically estimating the integral. The RMS difference between the analytical model results and the empirical test results is 0.02 evaluated over the range of  $\Omega_{I/S}$  tested empirically.

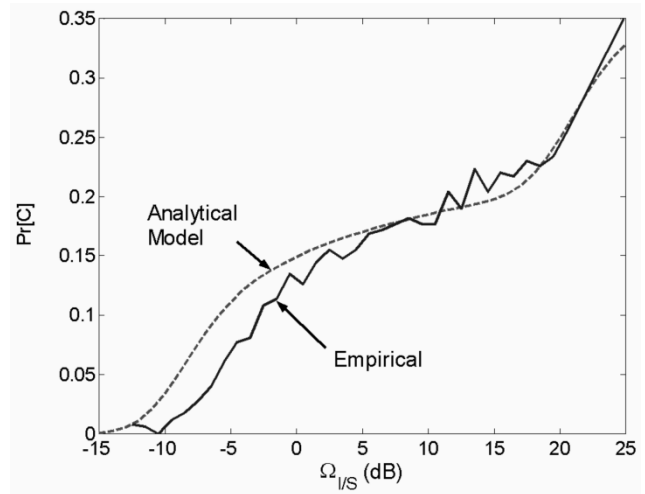


Fig. 8. Comparison between the analytical model and the empirical data for the  $\Pr[C]$  versus  $\Omega_{I/S}$  based on a single 802.11b interferer.

## V. COEXISTENCE IN A NETWORK INTERFERENCE ENVIRONMENT

In this section, the analytic model from Section IV is extended to provide a numerical estimate of  $\Pr[C]$  when a Bluetooth piconet is operating in an arbitrary 802.11b network environment.  $\Pr[C]$  is based on the number of 802.11b access points (APs) and the number of 802.11b stations (STAs) active, with their transmission time coincident and with sufficient power at the Bluetooth receiver to cause a collision. The topology for the coexistence scenario, assumed for the stochastic model development, was as follows. The transmitting Bluetooth node,  $BT_{TX}$  and receiving Bluetooth node,  $BT_{RX}$ , were located randomly within a workspace. The  $BT_{TX}$  and  $BT_{RX}$  were separated by distance  $d_S$ , as illustrated in Fig. 9. The APs of the 802.11b WLAN were iid within the workspace, as were the 802.11b STAs. The locations of the APs and STAs were independent. The nominal coverage range for the 802.11b APs was  $d_{AP}$ , as illustrated in the figure. Each AP supported an offered network traffic,  $G$ . The traffic was generated by both the AP in the downlink to the STAs within the APs' coverage area,  $\pi d_{AP}^2$ , as well as the uplink traffic from the STAs. The offered traffic was assumed to be the same at each AP and the uplink traffic was assumed to be equilikely from the STAs within the APs' coverage area.

For developing the single interferer analytical model,  $\Pr[C]$  was evaluated based on a given  $\Omega_{I/S}$  and therefore as indicated in (10)  $\Pr[C|\gamma, f_{\text{offset}}]$  is dependent on  $\gamma(f_{\text{offset}}) \leq \Omega_{I/S}$ . In order to facilitate the determination of  $\Pr[C]$  for the network interference environment, the RV  $\gamma(f_{\text{offset}})$  was divided into an ordered set of mutually exclusive events  $\gamma_l < \gamma(f_{\text{offset}}) \leq \gamma_{l+1}$  with  $\gamma_l < \gamma_{l+1} \forall l \in \mathfrak{S}$ . In this fashion, the conditional collision probability  $\Pr[C|\gamma_l < \gamma(f_{\text{offset}}) \leq \gamma_{l+1}]$  can be evaluated as presented below in (17) and (18) and by using the principle of total probability

$$\Pr[C] = \sum_{l=-\infty}^{\infty} \Pr[C|\gamma_l < \gamma(f_{\text{offset}}) \leq \gamma_{l+1}] \cdot \Pr[\gamma_l < \gamma(f_{\text{offset}}) \leq \gamma_{l+1}]. \quad (14)$$

Using the conditional pdf of  $\gamma(f_{\text{offset}})$  and the pdf of  $f_{\text{offset}}$  established in Section IV,

$$\Pr[C] = \sum_{l=-\infty}^{\infty} \Pr[C|\gamma_l < \gamma(f_{\text{offset}}) \leq \gamma_{l+1}] \cdot \int_{-B_{UL}/2}^{B_{UL}/2} \int_{\gamma_l}^{\gamma_{l+1}} f_{\gamma}(\gamma|f_{\text{offset}}) \cdot f_{f_{\text{offset}}}(f_{\text{offset}}) d\gamma df_{\text{offset}}. \quad (15)$$

Based on the same assumptions used to derive (12)

$$\Pr[C] = \frac{1}{B_{UL}} \sum_{l=-\infty}^{\infty} \Pr[C|\gamma_l < \gamma(f_{\text{offset}}) \leq \gamma_{l+1}] \cdot \int_0^{B_{UL}/2} \left[ \text{erfc}\left(\frac{\gamma_l - \bar{\gamma}(f_{\text{offset}})}{\sqrt{2}\sigma_{\gamma}}\right) - \text{erfc}\left(\frac{\gamma_{l+1} - \bar{\gamma}(f_{\text{offset}})}{\sqrt{2}\sigma_{\gamma}}\right) \right] df_{\text{offset}}. \quad (16)$$

Assuming the activity for each AP and each STA is iid, then  $\Pr[C|\gamma_l < \gamma(f_{\text{offset}}) \leq \gamma_{l+1}]$  can be approximated based on a bivariate binomial distribution over  $m$  and  $n$

$$\Pr[C|\gamma_l < \gamma(f_{\text{offset}}) \leq \gamma_{l+1}] \approx \sum_{m=0}^{N_{AP,l}} \sum_{n=0}^{N_{STA,l}} \binom{N_{AP,l}}{m} \binom{N_{STA,l}}{n} \times (\Pr[A_{AP}])^m (1 - \Pr[A_{AP}])^{N_{AP,l}-m} \cdot (\Pr[A_{STA}])^n (1 - \Pr[A_{STA}])^{N_{STA,l}-n} \cdot \Pr[C|m, n, \gamma_l < \gamma(f_{\text{offset}}) \leq \gamma_{l+1}] \quad (17)$$

where  $N_{AP,l}$  and  $N_{STA,l}$  are, respectively, the total number of APs and total number of STAs with  $\Omega_{I/S} \geq \gamma(f_{\text{offset}})$  given  $\gamma_l < \gamma(f_{\text{offset}}) \leq \gamma_{l+1}$ .  $\Pr[A_{AP}]$  and  $\Pr[A_{STA}]$  are, respectively, the probability of activity for the AP and STA. The technique used in determining  $N_{AP,l}$  and  $N_{STA,l}$  is derived in Section V-A. The conditional probability of collision given  $m$  and  $n$  active APs and STAs, respectively, and with  $\gamma_l < \gamma(f_{\text{offset}}) \leq \gamma_{l+1}$ , is similar to (10) (see (18) at the bottom of the page), where  $\Pr[C_T|m, n]$  is the probability the Bluetooth packet or acknowledgment is time coincident with any one of the active APs' or STAs' packets or acknowledgment.  $\Pr[C_T|m, n]$  is derived in Section V-B.

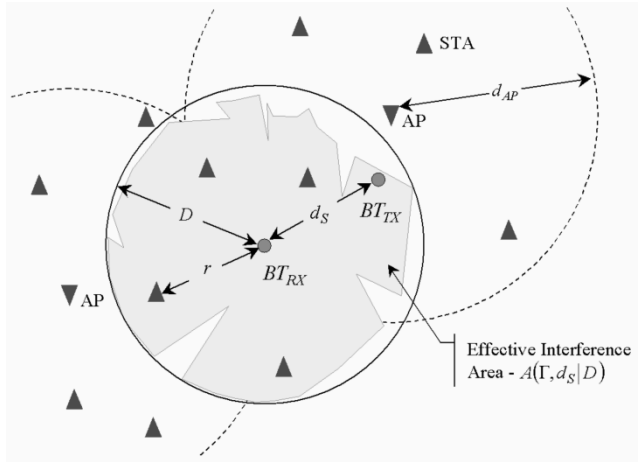


Fig. 9. Coexistence scenario topology and geometry for analyzing effective interference area.

The collision probability for an 802.11b network interference environment can be approximated by substituting (17) and (18) into (16),

$$\Pr[C] \approx \frac{1}{B_{UL}} \sum_{l=-\infty}^{\infty} \sum_{m=0}^{N_{AP,l}} \sum_{n=0}^{N_{STA,l}} \binom{N_{AP,l}}{m} \binom{N_{STA,l}}{n} \times (\Pr[A_{AP}])^m (1 - \Pr[A_{AP}])^{N_{AP,l}-m} \cdot (\Pr[A_{STA}])^n (1 - \Pr[A_{STA}])^{N_{STA,l}-n} \Pr[C_T|m, n] \times \int_0^{B_{UL}/2} \left[ \text{erfc}\left(\frac{\gamma_l - \bar{\gamma}(f_{\text{offset}})}{\sqrt{2}\sigma_{\gamma}}\right) - \text{erfc}\left(\frac{\gamma_{l+1} - \bar{\gamma}(f_{\text{offset}})}{\sqrt{2}\sigma_{\gamma}}\right) \right] df_{\text{offset}}. \quad (19)$$

Based on the results from Sections V-A and V-B, (19) is refined in Section V-C.

#### A. Expected Number of Interferers

The number of 802.11b AP and STA,  $N_{AP,l}$  and  $N_{STA,l}$ , respectively, with  $\Omega_{I/S} \geq \gamma(f_{\text{offset}})$  given  $\gamma_l < \gamma(f_{\text{offset}}) \leq \gamma_{l+1}$  is derived based on examining the relative received powers at the  $BT_{RX}$  from both the  $BT_{TX}$  and the 802.11b interferers within a radius  $D$  of the  $BT_{RX}$ , Fig. 9. The approach used is similar to the one derived by the author in [3]. Based on the APs and STAs being uniformly distributed with density  $D_{AP}$  AP/m<sup>2</sup> and  $D_{STA}$  STA/m<sup>2</sup>, respectively, then

$$\begin{aligned} N_{AP}(\Gamma_l) &= A_{\text{eff}}(\Gamma_l, d_S | D) D_{AP} \\ N_{STA}(\Gamma_l) &= A_{\text{eff}}(\Gamma_l, d_S | D) D_{STA} \end{aligned} \quad (20)$$

and

$$\begin{aligned} N_{AP,l} &= \text{round}(N_{AP}(\Gamma_l)) \\ N_{STA,l} &= \text{round}(N_{STA}(\Gamma_l)) \end{aligned} \quad (21)$$

$$\Pr[C|m, n, \gamma_l < \gamma(f_{\text{offset}}) \leq \gamma_{l+1}] = \begin{cases} \Pr[C_T|m, n] & [\Omega_{I/S} \geq \gamma(f_{\text{offset}}) | \gamma_l < \gamma(f_{\text{offset}}) \leq \gamma_{l+1}] \\ 0 & \text{o.w.} \end{cases} \quad (18)$$

where  $A_{\text{eff}}(\Gamma_l, d_S|D)$  is the effective area of interference given radius  $D$ .  $A_{\text{eff}}(\cdot)$  estimates the area within a circle centered at the  $BT_{RX}$  with radius  $D$  where the interference signal from the 802.11b AP and STA exceed the normalized interference to signal power ratio threshold,  $\Gamma_l$ .  $A_{\text{eff}}(\cdot)$  is also dependent on the distance between the  $BT_{TX}$  and the  $BT_{RX}$ ,  $d_S$ , where the dependency is governed by the radio propagation path loss characteristics. The normalized interference to signal power ratio threshold is

$$\Gamma_l = \frac{\gamma_l + \gamma_{l+1}}{2} + \Omega_{BT} - \hat{\Omega}_{802} \text{ (dB)} \quad (22)$$

where  $\Omega_{BT}$  is the Bluetooth transmit power in dBm.  $\hat{\Omega}_{802}$  is the 802.11b AP or STA power, within the passband of the  $BT_{RX}$ ,

$$\hat{\Omega}_{802} = \Omega_{802} - 10 \log_{10} \left( \frac{B_{802}}{B_{eq}} \right) \text{ (dBm)} \quad (23)$$

where  $\Omega_{802}$  and  $B_{802}$  are the 802.11b transmit power and bandwidth, respectively. Since 802.11b transmits a wideband DS/SS signal,  $B_{eq}$  was based on the Bluetooth equivalent noise bandwidth, [15]

$$B_{eq} = \int_0^\infty \frac{|H_{BT}(f)|^2 df}{\max |H_{BT}(f)|^2} \quad (24)$$

where  $H_{BT}(f)$  is the frequency response of the Bluetooth Gaussian filter. Using  $B \times T = 0.5$  [2], then  $B_{eq} = 0.81$  MHz.

The effective interference area was determined using an approach similar to Jake's method [16] for determining the percentage of the useful coverage area within a cell's boundary when taking into account the effects of shadowing. That is

$$A_{\text{eff}}(P_{TH}, d_S|D) = \int_0^{2\pi} \int_0^D \Pr(\Omega_I(r) - \Omega_S(d_S) > P_{TH}) \cdot r dr d\theta \quad (25)$$

where  $\Pr(\Omega_I(r) - \Omega_S(d_S) > P_{TH})$  is the probability the interference power,  $\Omega_I(r)$ , at radius  $r$ , exceeds the received signal power from the STA,  $\Omega_S(d_S)$ , by a power threshold  $P_{TH}$ . Both the signal power and interference power were based on a standard exponential decaying path loss model with path loss exponent,  $n$  and log-normal shadowing with standard deviations,  $\sigma_S$  and  $\sigma_I$ , respectively [17]. Assuming the log-normal distributed RVs used to model the shadowing for both the interference and the desired signal are independent, then the interference to signal ratio is

$$\begin{aligned} \Omega_{I/S}(r, d_S) &= \Omega_I(r) - \Omega_S(d_S) \\ &= \hat{\Omega}_{802} - \Omega_{BT} - 10n \log_{10} \left( \frac{r}{d_S} \right) - X_{I/S} \text{ (dB)} \end{aligned} \quad (26)$$

where  $X_{I/S}$  is a zero mean log-normal distributed RV with standard deviation  $\sigma_{I/S} = \sqrt{\sigma_I^2 + \sigma_S^2}$ . Using (26), (25) can be solved in a similar manner as the percentage coverage area as formulated in [18]

$$\begin{aligned} A_{\text{eff}}(\Gamma_l, d_S|D) &= \frac{\pi D^2}{2} \left[ 1 - \text{erf}(a) + \exp\left(\frac{1-2ab}{b^2}\right) \right. \\ &\quad \left. \cdot \left[ 1 - \text{erf}\left(\frac{1-ab}{b}\right) \right] \right] \end{aligned} \quad (27)$$

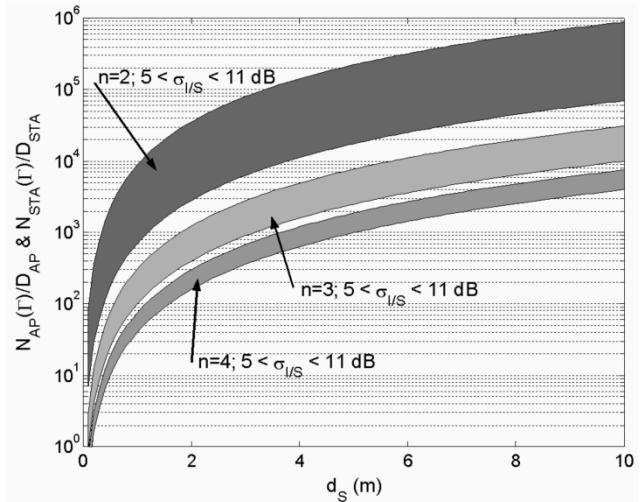


Fig. 10. Normalized number of 802.11b interferers, STAs and APs, exceeding interference threshold,  $\Gamma_l = -20.6$  dB, based on distance between the  $BT_{TX}$  and  $BT_{RX}$ .

where

$$a = \frac{\left( \frac{\gamma_l + \gamma_{l+1}}{2} - \bar{\Omega}_{I/S}(r, d_S) \right)}{\sqrt{2}} \sigma_{I/S} = \Gamma_l + 10n \log_{10} \left( \frac{r}{d_S} \right)$$

and  $b = (10n \log_{10} e) / \sqrt{2} \sigma_{I/S}$ . By letting  $D \rightarrow \infty$ ,

$$\begin{aligned} A_{\text{eff}}(\Gamma_l, d_S) &= \lim_{D \rightarrow \infty} A_{\text{eff}}(\Gamma_l, d_S|D) \\ &= \pi (d_S)^2 \exp \left[ \frac{2 \left( \sigma_{I/S}^2 - 10n \Gamma_l \log_{10}(e) \right)}{(10n \log_{10}(e))^2} \right], \end{aligned} \quad (28)$$

the area is based on the Bluetooth piconets satisfying  $\Omega_{I/S}(r, d_S) > (\gamma_l + \gamma_{l+1})/2$  regardless of  $D$ . Fig. 10 contains graphs for normalized number of 802.11b interferers,  $N_{AP}(\Gamma_l)/D_{AP} = N_{STA}(\Gamma_l)/D_{STA} = A_{\text{eff}}(\Gamma_l, d_S)$ , for  $\Gamma_l = -20.6$  dB. The parameter  $\Gamma_l$  was based on using typical transmit powers  $\Omega_{BT} = 0$  dBm and  $\Omega_{802} = 20$  dBm where  $\Omega_{802} = 20$  dBm corresponds to  $\hat{\Omega}_{802} = 6.6$  dBm. The power threshold  $(\gamma_l + \gamma_{l+1})/2 = -14$  dB was selected such that the graphs represent a reasonable upper limit for the normalized number of interferers when the signals are cochannel.

### B. Probability of Time Coincidence

From (18),  $\Pr[C_T|m, n]$  is the probability of time coincidence between the Bluetooth signal and 802.11b interference signal such that the Bluetooth packet requires retransmission, given  $m$  active APs and  $n$  active STAs with sufficient power to cause interference. The relative timing between Bluetooth and 802.11b is illustrated in Fig. 7. For the 802.11b, a packet transmission,  $T_P$ , from source to destination, is followed by an acknowledgment,  $T_{Ack}$ , from destination to source. A short interframe space,  $SIFS = 10 \mu\text{s}$ , occurs between  $T_P$  and  $T_{Ack}$ . The delay prior to the next transmission is random. Therefore, in the analytical model, a fixed value was used based on  $DIFS + E_{T_{bo}}$  where  $DIFS = 50 \mu\text{s}$  is the distributed coordination function interframe space and  $T_{bo}$  is the random backoff time interval,  $E[T_{bo}] \approx 300 \mu\text{s}$ .

TABLE II  
EVENTS AND CORRESPONDING PROBABILITIES THAT MODEL THE TIME COINCIDENCE BETWEEN A SINGLE 802.11b INTERFERER AND A BT PACKET

Probability	Event Description
$\Pr[C_{T,P} Ack] = \min\left(\frac{T_{Ack} + \tau_{BT}}{T_{802}}, 1\right)$	The 802.11b acknowledgement from either an AP or STA is time coincident with any part of the BT packet.
$\Pr[C_{T,H} Ack] = \min\left(\frac{T_{Ack} + \tau_H}{T_{802}}, 1\right)$	The 802.11b acknowledgement from either an AP or STA is time coincident with any part of the BT header and/or access code.
$\Pr[C_{T,P} Packet] = \min\left(\frac{T_P + \tau_{BT}}{T_{802}}, 1\right)$	The 802.11b packet from either an AP or STA is time coincident with any part of the BT packet.
$\Pr[C_{T,H} Packet] = \min\left(\frac{T_P + \tau_H}{T_{802}}, 1\right)$	The 802.11b packet from either an AP or STA is time coincident with any part of the BT header and/or access code.

For the 802.11b based on using a short preamble and header, the following times were indicated:  $T_P = 1210 \mu s$ ,  $T_{Ack} = 106 \mu s$  and  $T_{802} = 1676 \mu s$ . If either the 802.11b packet or acknowledgment is time coincident with the Bluetooth transmission, then a collision could occur. These two events were modeled as independent.

Data communications in the Bluetooth WPAN involves packet transmissions in either 1, 3 or 5 time slots from the source to the destination. In the time slot following the packet transmission, an acknowledgment is sent to the source from the destination. For Bluetooth, the acknowledgment is contained in the header of the packet. Therefore, two events can occur during a Bluetooth packet transmission that can result in a collision and thereby require a Bluetooth packet retransmission. Either the packet can be corrupted by 802.11b interference at the destination and/or the acknowledgment of the packet can be corrupted at the packet's source. These two events were modeled as being independent. This assumption is justified on two accounts. The Bluetooth packet and acknowledgment occur on different frequencies based on the Bluetooth frequency hopping pattern. In addition, the physical separation between the Bluetooth receiver and transmitter will lead to a decrease in the correlation between the interference at each node. The following times were used for Bluetooth:  $\tau_H = 126 \mu s$  and  $\tau_{BT} = 366, 1616, 2866 \mu s$  corresponding respectively to nominal maximum transmission times for 1, 3 and 5 slot packet types.

Letting the RV  $\tau_{\text{offset}}$  represent the relative time offset between an 802.11b frame and the Bluetooth transmission, four independent events can occur. These events and corresponding

probabilities are given in Table II. Using results from Table II, the conditional probabilities of temporal coincidence given a single 802.11b interferer is transmitting either an acknowledgment or a packet are

$$\begin{aligned} \Pr[C_T|Ack] &= \Pr[C_{T,P}|Ack] + \Pr[C_{T,H}|Ack] \\ &\quad - \Pr[C_{T,P}|Ack] \Pr[C_{T,H}|Ack] \\ \Pr[C_T|Packet] &= \Pr[C_{T,P}|Packet] + \Pr[C_{T,H}|Packet] \\ &\quad - \Pr[C_{T,P}|Packet] \Pr[C_{T,H}|Packet]. \end{aligned} \quad (29)$$

For the single time slot Bluetooth packet,  $\Pr[C_T|Ack] = 0.38$  and  $\Pr[C_T|Packet] = 0.99$ . For the 3 and the 5 slot Bluetooth packets, both conditional probabilities are 1.0.

In order to model the imbalance between 802.11b downlink and uplink traffic,  $R$  is used to denote the probability of downlink packet transmission. Using (29) and assuming independence between the  $m$  APs and  $n$  STAs, then a joint binomial distribution can be used to evaluate  $\Pr[C_T|m, n]$ . This is based on summing the individual conditional collision probabilities that occur when  $j$  out of the  $m$  APs send packets,  $i$  out of the  $n$  STAs send packets and the remaining active interferers are sending acknowledgment, i.e.,

$$\begin{aligned} \Pr[C_T|m, n] &= 1 - \left[ \sum_{i=0}^n \sum_{j=0}^m \binom{n}{i} \binom{m}{j} R^{j+(n-i)} (1-R)^{i+(m-j)} \right. \\ &\quad \times (1 - \Pr[C_T|Ack])^{(n-i)+(m-j)} \\ &\quad \left. \cdot (1 - \Pr[C_T|Packet])^{i+j} \right]. \end{aligned} \quad (30)$$

### C. Probability of Collision

The  $\Pr[C]$  for the 802.11b network interference environment is evaluated using (19), based on (21) to evaluate  $N_{AP,l}$  and  $N_{STA,l}$  and based on (30) to evaluate  $\Pr[C_T|m, n]$ . By factoring terms, after substituting (30) into (19) and then with repeated application of the identity,  $(a+b)^n = \sum_{j=0}^n \binom{n}{j} b^j a^{n-j}$ , a simplified version of (19) is obtained, as shown in (31) at the bottom of the page. The  $\Pr[A_{AP}]$  and  $\Pr[A_{STA}]$  are obtained based on the assumptions used in modeling the 802.11b network outlined in the introduction to Section V. From Section V-B, an active interferer, AP or STA, indicates the interferer is transmitting either an

$$\begin{aligned} \Pr[C] &\approx \frac{1}{B_{UL}} \sum_{l=-\infty}^{\infty} \left\{ \left[ 1 - \left( (R \Pr[C_T|Packet] + (1-R) \Pr[C_T|Ack]) \Pr[A_{AP}] \right)^{N_{AP,l}} \right. \right. \\ &\quad \times \left. \left. \left( 1 - (R \Pr[C_T|Ack] + (1-R) \Pr[C_T|Packet]) \Pr[A_{STA}] \right)^{N_{STA,l}} \right] \right. \\ &\quad \left. \times \int_0^{B_{UL}/2} \left[ \operatorname{erfc} \left( \frac{\gamma l - \bar{\gamma}(f_{\text{offset}})}{\sqrt{2}\sigma_\gamma} \right) - \operatorname{erfc} \left( \frac{\gamma l + 1 - \bar{\gamma}(f_{\text{offset}})}{\sqrt{2}\sigma_\gamma} \right) \right] df_{\text{offset}} \right\}. \end{aligned} \quad (31)$$



acknowledgment frame or a packet frame. Therefore, for the AP,

$$\Pr[A_{AP}] = \min[G, 1] \quad (32)$$

where  $G$  was defined as the offered traffic to a given AP within the network. Since each STA within the coverage area of the AP is equilikely, then

$$\Pr[A_{STA}] = \min\left[\frac{G}{D_{STA}\pi d_{AP}^2}, 1\right]. \quad (33)$$

The relationship between the analytical models' for the single 802.11 interferer, (12) and the 802.11 network environment, (31), can be obtained by letting  $R = 1$ ,  $\Pr[A_{AP}] = 1$  and  $\Pr[C_T|Ack] = 0$ , then (31) reduces to

$$\Pr[C] \approx \frac{1}{B_{UL}} \sum_{l=-\infty}^{\infty} \left\{ 1 - (1 - \Pr[C_T|Packet])^{N_{AP,l}} \times \int_0^{B_{UL}/2} \left[ \operatorname{erfc}\left(\frac{\gamma_l - \bar{\gamma}(f_{\text{offset}})}{\sqrt{2}\sigma_\gamma}\right) - \operatorname{erfc}\left(\frac{\gamma_{l+1} - \bar{\gamma}(f_{\text{offset}})}{\sqrt{2}\sigma_\gamma}\right) \right] df_{\text{offset}} \right\}. \quad (34)$$

By letting

$$N_{AP,l} = \begin{cases} 1 & \Omega_{I/S} \geq \frac{\gamma_{l+1} + \gamma_l}{2}, \\ 0 & \text{o.w.} \end{cases}, \quad (35)$$

then

$$\Pr[C] \approx \frac{\Pr[C_T|Packet]}{B_{UL}} \cdot \sum_{l=-\infty}^L \int_0^{B_{UL}/2} \left[ \operatorname{erfc}\left(\frac{\gamma_l - \bar{\gamma}(f_{\text{offset}})}{\sqrt{2}\sigma_\gamma}\right) - \operatorname{erfc}\left(\frac{\gamma_l + \varepsilon_\gamma - \bar{\gamma}(f_{\text{offset}})}{\sqrt{2}\sigma_\gamma}\right) \right] df_{\text{offset}} \quad (36)$$

where  $L = \arg \min_{l \in \mathfrak{S}} [\gamma_l + \varepsilon_\gamma \Omega_{I/S}]$  and  $\varepsilon_\gamma = (\gamma_{l+1} - \gamma_l)/2 \forall l \in \mathfrak{S}$ . Then in the limit, as  $\varepsilon_\gamma \rightarrow 0$  (12) and (36) are equivalent. For the analysis presented in Section VI,  $\varepsilon_\gamma = 1$  dB.

## VI. COEXISTENCE ANALYSIS

The Bluetooth  $E[PER]$  in the presence of 802.11b interference is evaluated under various network and radio propagation environments based on (2) and (31). There are essentially seven independent variables associated with evaluating (31), which can be grouped into two sets of parameters:

- 1) 802.11b network parameters:  $V_{802} = [G, R, D_{STA}, d_{AP}]'$
- 2) Radio propagation parameters:  $V_R = [n, \sigma_{I/S}, d_s]'$

The parameter  $D_{AP} = 1/(\pi d_{AP}^2)$ , i.e., the density of the APs, is directly related to the APs coverage area. The overall parameter space is then represented by  $V = \begin{bmatrix} V_{802} \\ V_R \end{bmatrix}$ . Not all the parameters are equally important in determining  $\Pr[C]$ . In order

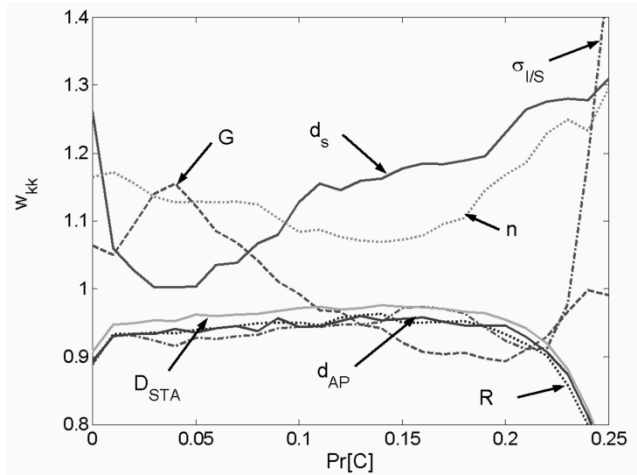


Fig. 11. Weighting factors for 802.11b network parameters and radio propagation parameters used to categorize parameter importance in determining  $\Pr[C]$ .

to obtain a measure of the dependency of  $\Pr[C]$  on each parameter, a technique similar to feature ordering, as presented in [19], is used.

A specific point in parameter space,  $v^i \in V$ , can be used to evaluate the collision probability,  $\Pr[C|v^i]$ , by evaluating (31). The intraset distance [19],  $\overline{D^2}$ , for a set of parameter points  $\{v^i, i = 1, \dots, K\}$  is given by

$$\overline{D^2} = 2 \sum_{k=1}^7 \sigma_k^2 \quad (37)$$

where  $\sigma_k^2$  is the unbiased sample variance of the  $k$ th parameter over the  $K$  parameter points; i.e.,

$$\sigma_k^2 = \frac{1}{K-1} \sum_{i=1}^K (v_k^i - \bar{v}_k)^2 \quad (38)$$

and

$$\bar{v}_k = \frac{1}{K} \sum_{i=1}^K v_k^i. \quad (39)$$

A weighting function is then found that ranks the importance of each parameter in influencing the category of the set of  $K$  parameter points. The weighting function is a transformation on the parameter space, such that the intraset distance in the transformed parameter space is minimized under the constraint  $\prod_{k=1}^7 w_{kk} = 1$  where  $W_{kk}$  is the weighting factor for the  $k$ th parameter. As derived in [19], the weighting factors based on the constraint are

$$w_{kk} = \frac{1}{\sigma_k} \left( \prod_{j=1}^7 \sigma_j \right)^{1/7}. \quad (40)$$

The weighting factor is inversely proportional to the sample standard deviation of the  $k$ th parameter. This technique is applied to categorize the parameters over the parameter points based on  $\{v^i | \xi_i \leq \Pr[C|v^i] < \xi_{i+1}\}$ .

A graph of  $w_{kk}$  with  $\{v^i | \xi_i \leq \Pr[C|v^i] < \xi_{i+1}, \xi_i \in [0, 0.01, 0.02, \dots, 1]\}$  is presented in Fig. 11. The results in the graph were based on evaluating (31) for dh1 Bluetooth packet type over a parameter space as defined by the parameter ranges in Table I. The motivation in selecting the parameter ranges was

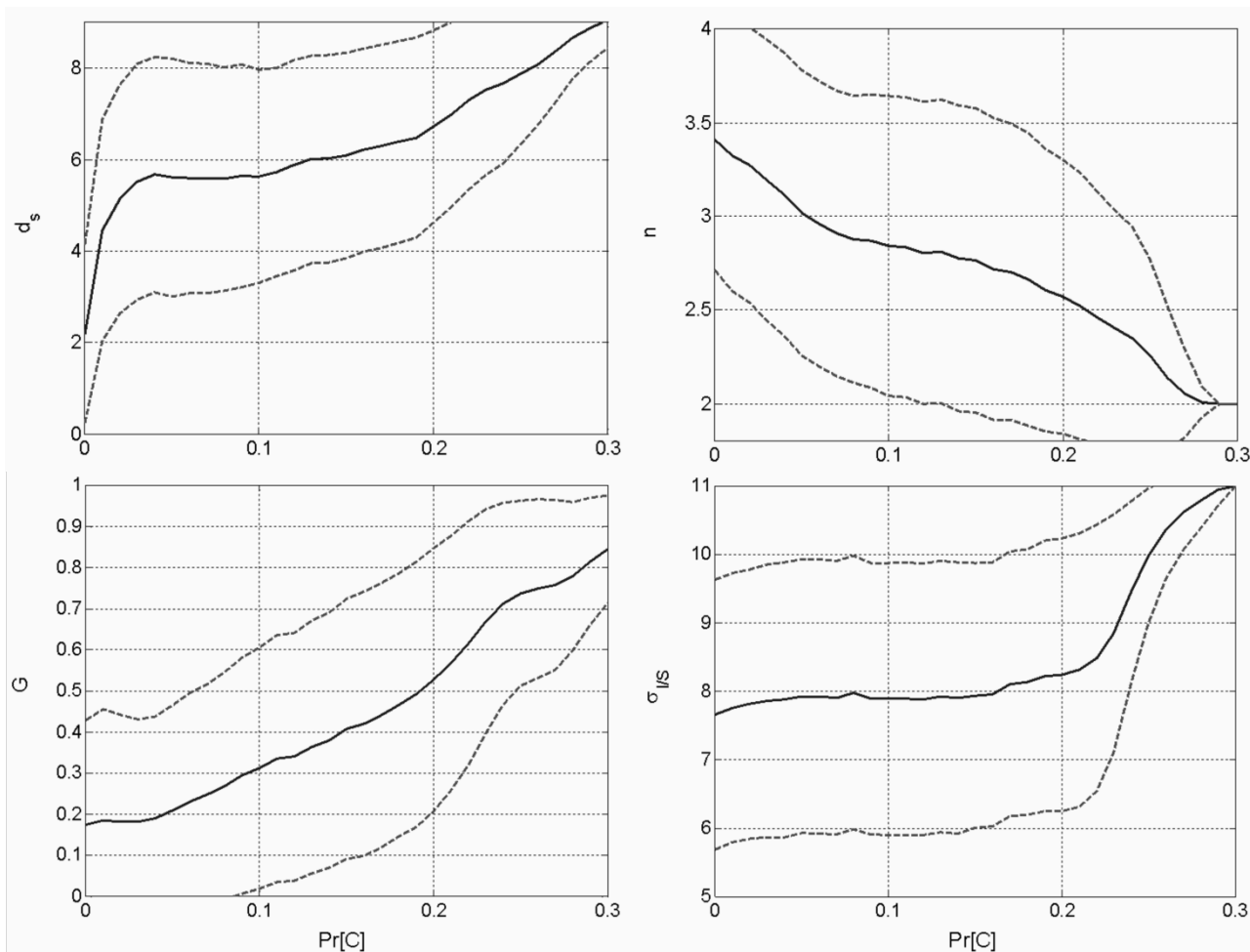


Fig. 12. Graphs of the sample mean, solid line, for four the seven parameters used in evaluating  $\Pr[C]$ . Dashed lines represent  $\pm\sigma$  about the mean.

to perform the analysis over a very board parameter space to assist in providing insight into the scenarios where 802.11b interference may or may not be an issue. The 802.11b network parameters are representative of the following interference environments:

- $G \in [0.01\ 1]$ Erlang—Each AP supports sustained data rates between 9 to 900 kbytes/s based on 1500 bytes/packet and  $T_{802} = 1676\ \mu\text{s}$ .
- $R \in [0\ 1]$ —No packet traffic on the downlink to all packet traffic on the downlink.
- $D_{STA} \in [0.02\ 0.1]$  STA/m<sup>2</sup>—On average 2 STA in a 100 m<sup>2</sup> area to 1 STA in a 10 m<sup>2</sup> area.
- $d_{AP} \in [15\ 20]$  m—Based on the nominal 802.11b maximum coverage range of 20 m for 11 Mbps data rate.

The radio propagation parameter ranges  $n \in [2\ 4]$  and  $\sigma_{I/S} \in [5\ 11]$  dB represent typical propagation parameters for indoor environments [18] and  $d_s \in [0.5\ 9.5]$  m represents the Bluetooth coverage range given a transmit power of 0 dBm. The sample mean, (39) and  $\pm\sigma$ , (38), about the mean, are graphed in Fig. 12 for four of the seven parameters. The graph for parameter  $D_{STA}$ ,  $d_{AP}$  and  $R$  were excluded, since their mean and variance were essentially constant over  $\Pr[C]$ . The nominal mean and standard deviation ( $\bar{v}_k, \sigma_k$ ) for these three parameters were  $D_{STA}(0.06, 0.03)$  STA/m<sup>2</sup>,  $d_{AP}(17.2, 1.6)$  m and  $R(0.49, 0.34)$ . As evident from Figs. 11 and 12,  $n$  and  $d_s$

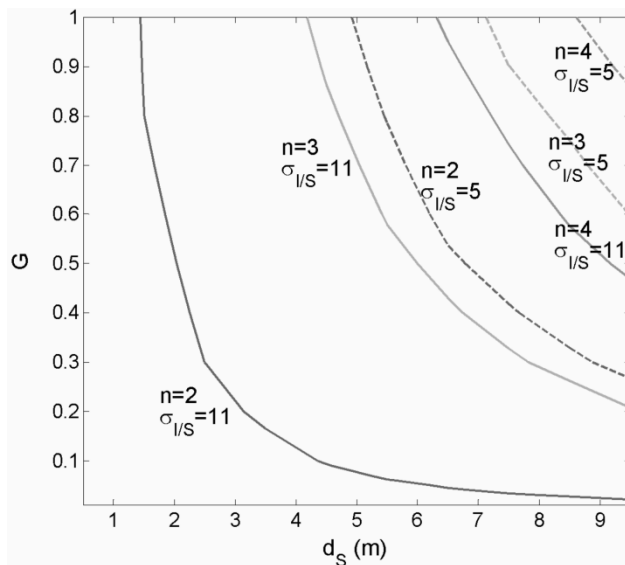


Fig. 13. Curves for  $\Pr[C] = 0.08$ , based on variations of four parameters, with  $R = 0.6$ ,  $D_{STA} = 0.06$  STA/m<sup>2</sup> and  $d_{AP} = 18$  m.

are significant in categorizing  $\Pr[C]$  over the entire range of  $\Pr[C]$ , whereas  $G$  and  $\sigma_{I/S}$  contribute significantly over specific ranges of  $\Pr[C]$ .

Figs. 13 and 14 depict contours of equal probability,  $\Pr[C] = 0.08$  and  $\Pr[C] = 0.2$ , respectively, over the ranges for the four

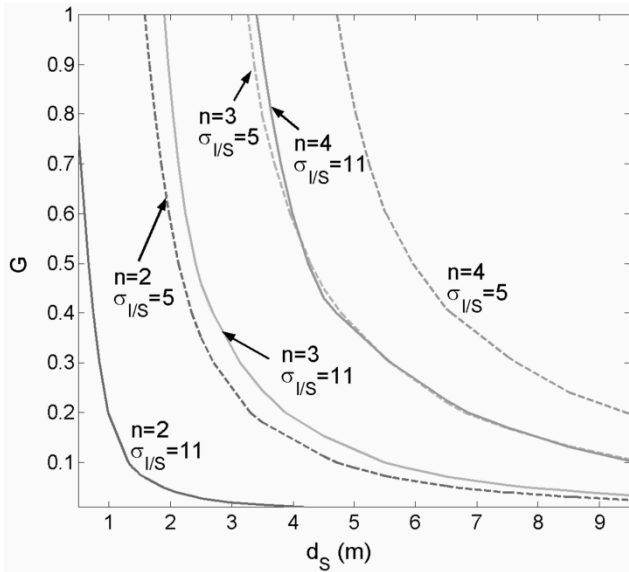


Fig. 14. Curves for  $\Pr[C] = 0.2$ , based on variations of four parameters, with  $R = 0.6$ ,  $D_{STA} = 0.06$  STA/m<sup>2</sup> and  $d_{AP} = 18$  m.

dominate parameters. For both graphs  $R$ ,  $D_{STA}$  and  $d_{AP}$  were set to  $R = 0.6$ ,  $D_{STA} = 0.06$  STA/m<sup>2</sup> and  $d_{AP} = 18$  m.

Motivated by the results depicted in Figs. 13 and 14, the conditional sample mean for the  $\Pr[C]$ ,  $E[\Pr[C]|n, d_s, G]$  was examined. The conditioning was based on evaluating  $G$  over two ranges of 802.11b network activity: light network activity,  $0.01 \leq G \leq 0.09$  (9 to 80 kbytes/s) and moderate to heavy network activity  $0.1 \leq G \leq 1$  (90 to 900 kbytes/s). The variation in the other four parameters,  $D_{STA}$ ,  $d_{AP}$ ,  $R$  and  $\sigma_{I/S}$ , are specified in Table I. Graphs of the resulting expectations are given in Fig. 15. Based on the graphs, the following observations are made:

- 1) For light 802.11b network activity, the Bluetooth piconet should not encounter any significant performance impact over its operational coverage range given the path loss is sufficiently large  $n \geq 3$ .
- 2) For moderate to heavy 802.11b network activity, it is likely that the Bluetooth piconet will encounter a limitation of its communication range between piconet nodes. The degree to which the range is limited is highly dependent on the path loss associated with the RF environment and the application's communication requirements, i.e., MOP criteria.

The results presented are based on the assumption that all 802.11b APs and STAs are operating on the same carrier frequency and within the same frequency band. If multiple APs are deployed in the same workspace, then it is likely, the APs would operate on up to three different, nonoverlapping frequency bands. This factor was not considered in the analysis, but could be examined with a straightforward extension to (31).

## VII. CONCLUSIONS

A method for analytically evaluating the impact an 802.11b will have on the Bluetooth piconet performance was developed. The analytical model for a single 802.11b interferer was evaluated against empirical test results with an RMS difference of

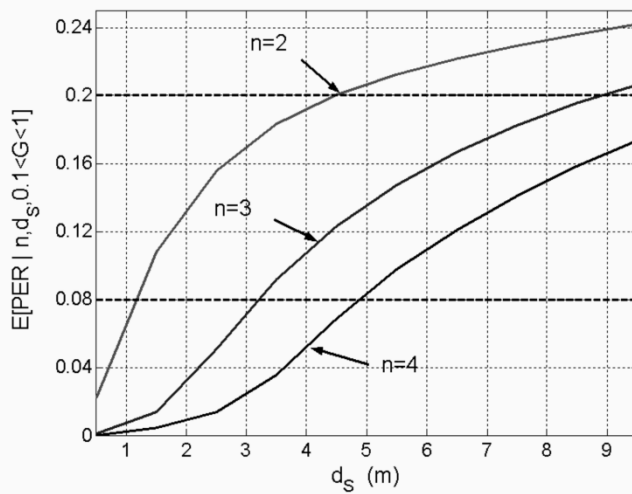
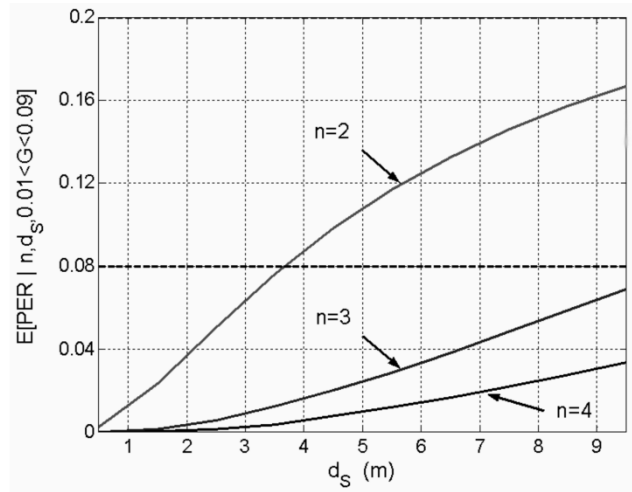


Fig. 15. Sample mean for the  $\Pr[C]$ , based on light 802.11b traffic constraint and moderate to heavy 802.11b traffic constraint.

2%. The single interferer analytical model was extended to enable evaluating Bluetooth performance in an arbitrary 802.11b network environment defined by two sets of parameters: 802.11b network parameters and radio propagation parameters. Analysis results are presented based on a very broad parameter space encompassing large variations in potential scenarios in which Bluetooth devices may operate. Based on this analysis two general conclusions are drawn.

- 1) For light 802.11b network activity, the Bluetooth piconet should not encounter any significant performance impact over its operational coverage range given the path loss is sufficiently large  $n \geq 3$ .
- 2) For moderate to heavy 802.11b network activity, it is likely that the Bluetooth piconet will encounter a limitation of its communication range between piconet nodes. The degree to which the range is limited is highly dependent on the path loss associated with the RF environment and the application's communication requirements, i.e., MOP criteria.

The overall methodology presented is applicable to a wide range of network configurations and network performance criteria. The conclusions drawn based on the analysis presented could be dramatically different, dependent on the parameter

ranges investigated. By tailoring the parameter space and the MOP criteria applied to the analysis, the coexistence issue can be investigated based on a given application's requirements.

#### ACKNOWLEDGMENT

The author would like to express his thanks to Mr. V. Mitter for conducting the empirical tests.

#### REFERENCES

- [1] J. C. Haartsen, "The bluetooth radio system," *IEEE Personal Communications*, vol. 7, pp. 28–36, 2000.
- [2] "Specification of the Bluetooth System v1.1," Bluetooth SIG, 2001.
- [3] I. Howitt, "WLAN and WPAN coexistence in UL band," *Transactions on Vehicular Technology*, vol. 50, pp. 1114–1124, 2001.
- [4] T. M. Siep, I. C. Gifford, R. C. Braley, and R. F. Heile, "Paving the way for personal area network standards: An overview of the IEEE P802.15 working group for wireless personal area networks," *IEEE Personal Communications*, vol. 7, pp. 37–43, 2000.
- [5] G. Ennis, "Impact of Bluetooth on 802.11 direct sequence," *IEEE P802.11-98/319*, 1998.
- [6] J. Zyren, "Extension of Bluetooth and 802.11 direct sequence interference model," *IEEE 802.11-98/378*, 1998.
- [7] —, "Reliability of IEEE 802.11 hi rate DSSS WLAN's in a high density Bluetooth environment," in Bluetooth '99, 1999.
- [8] J. C. Haartsen and S. Zürbes, *Bluetooth Voice and Data Performance in 802.11 DS WLAN Environment*: Ericsson Sig Publication, 1999.
- [9] A. Kamerman, "Coexistence between Bluetooth and IEEE 802.11 CCK solutions to avoid mutual interference," *IEEE 802.11-00/162*, 2000.
- [10] R. V. Hogg and E. A. Tanis, *Probability and Statistical Inference*. New York: MacMillan, 1977.
- [11] A. Papoulis, *Probability, Random Variables and Stochastic Processes*, 2nd ed. New York: McGraw-Hill, 1984.

- [12] I. Howitt, "IEEE 802.11 and Bluetooth coexistence methodology," in *IEEE Spring VTC 2001*, vol. 2, Rhodes, 2001, pp. 1114–1118.
- [13] M. Webster and K. Halford, "Suggested PA model for 802.11 HRB," *IEEE 802.11-00/294*, September 2000.
- [14] W. Press, S. Teukolsky, W. Vetterling, and B. Flannery, *Numerical Recipes in C*, 2nd ed., 1992.
- [15] J. Proakis, *Digital Communications*, 3rd ed, NY: McGraw-Hill, 1995.
- [16] W. C. Jakes, *Microwave Mobile Communications*: Wiley-Interscience, 1974.
- [17] G. Stüber, *Principles of Mobile Communication*: Kluwer, 1996.
- [18] T. S. Rappaport, *Wireless Communications Principles and Practice*. New York: IEEE Press & Prentice Hall PTR, 1996.
- [19] J. T. Tou and R. C. Gonzalez, *Pattern Recognition Principles*: Addison-Wesley, 1974.



**Ivan Howitt** (M'84) received the B.E.E. and M.S.E.E. degrees from Georgia Institute of Technology, Atlanta, in 1982 and 1990, respectively, and the Ph.D. degree in electrical engineering from University of California, Davis, in 1995.

From 1982 to 1990, he was a Research Engineer with Georgia Tech Research Institute. In 1995 to 1996, he was a Visiting Assistant Professor at Virginia Tech and a research associate at the Mobile and Portable Radio Research Group (MPRG). From 1996 to 2002, he was an Assistant Professor in the Department of Electrical Engineering & Computer Science, University of Wisconsin, Milwaukee. In 2002, he joined the Department of Electrical & Computer Engineering, University of North Carolina, Charlotte (UNCC) as an Associate Professor. His research interests include interoperability issues facing UL band wireless services, methods for mitigating interference, and approaches for optimizing wireless network performance.